Acknowledgment

A portion of this work was sponsored by the United States Air Force Office of Scientific Research under Contract F49620–92-C-0006.

References

[1]Malik, M., Zang, T., and Bushnell, D., "Boundary Layer Transition in Hypersonic Flows," AIAA Paper 90-5232, Oct. 1990.

[2]Fedorov, A. V., Gushchin, V. R., and Tumin, A. M., "Transition to Turbulence on Hypersonic Vehicles," *Proceedings of the ASME Fluid Engineering Conference* (Washington, DC), *Turbulent Flows—1993*, FED-Vol. 155, American Society of Mechanical Engineers, 1993, pp. 55–58.

[3]Malmuth, N. D., "Stability of the Inviscid Shock Layer in Strong Interaction Flow over a Hypersonic Flate Plate," *Instabilities and Turbulence in Engineering Flows*, Fluid Mechanics and Its Applications Series, Kluwer, Dordrecht, The Netherlands, 1993, pp. 189–223.

[4]Wright, R. L., and Zoby, E. V., "Flight Boundary Layer Transition Measurements on a Slender Cone at Mach 20," AIAA Paper 77-719, June 1977.

[5]Mack, L. M., "Boundary Layer Stability Theory," Jet Propulsion Lab., Doc. 900-277, Rev. A, Pasadena, CA, 1969.

[6]Fedorov, A., and Malmuth, N., "Analysis of Similarity Methods in Hypersonic Transition Prediction," Rockwell International Science Center, Rept. RISC94NM2, Thousand Oaks, CA, Aug. 1994.

[7]Hayes, W. D., and Probstein, R. F., *Hypersonic Flow Theory*, Academic, New York, 1959.

Vortex Development over Flat Plate Riblets in a Transitioning Boundary Layer

J. A. Rothenflue* and P. I. King†
U.S. Air Force Institute of Technology, Wright–Patterson Air Force Base, Ohio 45433

Introduction

THE majority of riblet research has focused on the reduction of turbulent boundary layer (TBL) skin-friction drag on a flat plate at zero pressure gradient.[1] For example, Choi[2] showed that riblets constrain the spanwise movement of the longitudinal vortices that exist just above the laminar sublayer. Current research by the authors is aimed at investigating potential applications for riblets in other than turbulent boundary layers.

For this research, riblets were placed in an incompressible, flat plate, zero-pressure-gradient boundary layer developing from a laminar to turbulent state. A three-component laser-Doppler anemometer was used to obtain velocity profiles within and above the riblets at several streamwise locations. Results indicate that riblets initiate the development of paired, streamwise vortices during boundary-layer transition. These vortices remain in place as they extend downstream and appear to evolve into the TBL vortical structures detected by Suzuki and Kasagi.[3]

Experimental Setup

The wind tunnel for this investigation consists of an air supply system, stilling chamber, and an enclosed test section that exhausts into a vented room. A flat test plate splits the test section from top to bottom, creating two separate 8 × 40 cm channels. Outer test section walls are adjustable to allow a zero pressure gradient along the length of the center plate. The freestream turbulence intensity entering the test section varies from 1.0 to 1.7%, depending on the freestream velocity.

Received Sept. 26, 1994; revision received March 31, 1995; accepted for publication April 3, 1995. This paper is declared a work of the U.S. Government and is not subject to copyright protection in the United States.

*Doctoral Candidate, ENA433. Member AIAA.

†Associate Professor, ENY, 2950 P Street. Senior Member AIAA.

V-groove riblets used for this investigation were machined into the Plexiglas test plate with 3.0-mm peak-to-peak width and 2.6-mm valley-to-peak height. The local u velocity component is defined parallel to the test plate in the streamwise direction, the v component normal to and away from the plate, and the w component parallel to the plate in the cross-stream direction, consistent with a right-handed coordinate system.

A DANTEC fiber flow three-axis laser-Doppler anemometry system was used in cross-coupled mode (off-axis backscatter), resulting in an approximately ellipsoidal probe volume measuring roughly 150 × 150 × 215 μm in size.

Results

Boundary-layer profiles were obtained over riblet valleys and peaks. In addition, spanwise velocity profiles over two riblets were taken at stations 0.5 and 3.0 mm above the riblet peaks. All profiles were obtained for three freestream velocities ($U \cong 3.5$, 7.5, and 15.0 m/s) and five streamwise stations on the plate ($x = 105$, 200, 300, 400, and 500 mm from the leading edge).

The state of the boundary layer (laminar, transitional, or turbulent) was determined from the distribution of turbulence intensity, given by $Tu = [(u_{\text{rms}}^2 + v_{\text{rms}}^2 + w_{\text{rms}}^2)/3]^{1/2} \times (1/U)$, as illustrated in Fig. 1. For the laminar boundary layer at $x = 105$ mm, the difference in turbulence intensity between the boundary layer and the freestream was negligible. In the transitional boundary layer at $x = 300$ mm, the elevated peak turbulence intensity within the boundary layer increased in the streamwise direction, until, for the fully turbulent boundary layer at $x = 500$ mm, the peak turbulence intensity remained constant. The arithmetic mean of two separate rms estimates, each based on 1000 Doppler bursts, was used to obtain Tu. For $U \cong 7.5$ m/s in Fig. 1, transition was first detected at $x = 200$ mm and was complete at $x = 400$ mm. For $U \cong 15.0$ m/s, transition began at $x \cong 105$ mm and was complete at $x = 400$ mm. Both of these cases correspond well with transition criteria given by Granville.[4] For the $U \cong 3.5$ m/s case however, transition began at $x \cong 300$ mm, earlier than the Granville prediction, and remained transitional up to the test section exit at $x = 500$ mm.

For all velocities, a pair of counter-rotating vortices developed within the riblet valleys downstream of initiation of transition. For this work, the vortices were first detected at $x = 500$ mm for $U \cong 3.5$ m/s, $x = 300$ mm for $U \cong 7.5$ m/s, and $x = 200$ mm for $U \cong 15.0$ m/s. Figures 2–4 include measurements at $x = 300$ mm, a location of transitional flow for all cases. At this x station, the 99% boundary-layer thickness was approximately 5.5 mm above the riblet peaks for $U \cong 3.5$ m/s and 4.5 mm for both $U \cong 7.5$ and 15.0 m/s. In these figures, each point is the arithmetic mean of the data from two passes, and each individual mean velocity measurement is the residence time-weighted mean of 1000 Doppler bursts. The 90% confidence intervals in the figures are based on the observed scatter in the data from the two passes and are representative for all data in the figure. Velocity confidence intervals never exceed ±0.4% of the freestream velocity.

Figure 2 shows the v velocity profiles over a riblet peak and valley, with the y datum at the bottom of the valley. It depicts a region of ascending particles above the peak and descending particles within the valley for $U \cong 7.5$ m/s and 15.0 m/s. Figures 3 and 4 are spanwise v and w profiles, respectively, spanning two complete riblets 0.5 mm

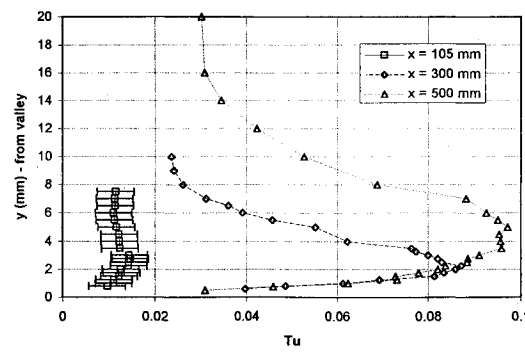

Fig. 1 Boundary layer Tu profiles, $U = 7.5$ m/s.

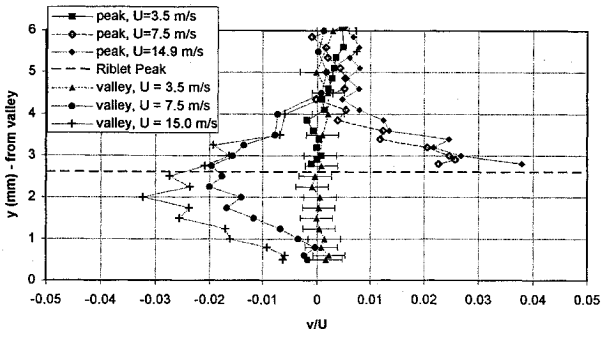

Fig. 2 Peak and valley v/U profiles, x = 300 mm.

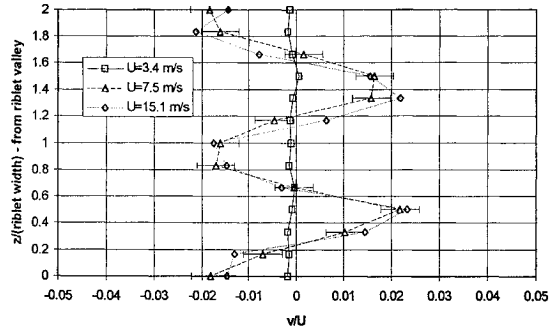

Fig. 3 Spanwise v-velocity profiles, y = 0.5 mm above peak, x = 300 mm.

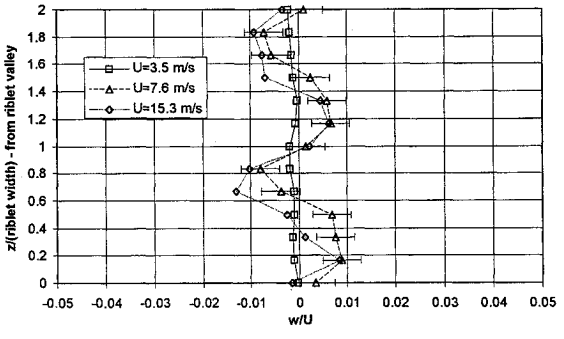

Fig. 4 Spanwise w-velocity profiles, y = 0.5 mm above peak, x = 300 mm.

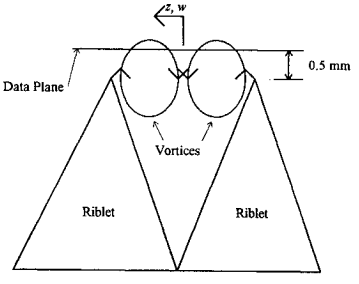

Fig. 5 Sketch of vortices within riblet valley.

above the peaks. The z parameter is the spanwise distance divided by the riblet spacing, with the datum directly over a riblet valley. Figure 3 shows a spanwise periodic pattern of ascending and descending particles just above the riblets. Paired vortical motion is confirmed in Fig. 4, which shows spanwise periodic patterns of alternating w velocities, with wavelength equal to the riblet spacing and offset in phase from the v profiles by 90 deg. The signs of the w velocities indicate that the vortex cores lie below the plane of data acquisition, as illustrated in Fig. 5. There was no significant vortical motion for the low speed case at x = 300 mm.

An inspection of all data obtained reveals that the vertical velocity component v was detected before (<100 mm upstream of) the spanwise component w, and both components are always $\lesssim$4% of the freestream velocity. Once formed, the vortices appear to maintain a constant position within the riblet profile. Finally, in the fully turbulent region for $U \cong$ 7.5 and 15.0 m/s, the maximum v/U and w/U components were similar in magnitude and approximately equal to 0.04.

Conclusions

Three-dimensional measurements of air velocity within and above riblets indicate the evolution of counter-rotating pairs of vortices during transition to turbulent flow. These vortices extend slightly above the riblet peaks and, once fully developed, maintain a constant location within the riblet profile with component velocities up to 4% of the freestream velocity. The vortices remain intact and of constant size downstream into the fully turbulent boundary-layer region.

References

[1]Walsh, M. J., "Riblets," *Viscous Drag Reduction in Boundary Layers*, edited by D. M. Bushnell and J. N. Heffner, Vol. 123, Progress in Astronautics and Aeronautics, AIAA, Washington, DC, 1990, pp. 203–261.

[2]Choi, K.-S., "Near Wall Structure of a Turbulent Boundary Layer with Riblets," *Journal of Fluid Mechanics*, Vol. 208, Nov. 1989, pp. 417–458.

[3]Suzuki, Y., and Kasagi, N., "Turbulent Drag Reduction Mechanism Above Riblet Surface," *AIAA Journal*, Vol. 32, No. 9, 1994, pp. 1781–1790.

[4]Schlichting, H., *Boundary Layer Theory*, 7th ed., McGraw–Hill, New York, 1979, p. 480.

Magnitude of Artificial Dissipation for Numerical Simulations

Y. Kallinderis* and H. McMorris†
University of Texas at Austin, Austin, Texas 78712

I. Introduction

A COMMON method for stabilizing numerical solutions is the addition of artificial dissipation. It is employed in order to suppress solution oscillations, as well as to capture shock waves with central-differencing numerical schemes.[1] This is usually achieved via a combination of second and fourth differences. The former is employed for shock capturing, whereas the latter is used for suppression of the odd-even modes of the numerical solution.[2] The amount of smoothing depends on ad hoc coefficients that are chosen a priori and remain the same during the computation. Artificial dissipation frequently results in severe deterioration of numerical accuracy, and especially so in cases of viscous flow simulations. Contamination of boundary-layer profiles due to smoothing is quite common.[3]

A simple method is proposed in the present work in order to calculate specific values of the smoothing coefficient that also result in a bounded amount of dissipation. The main differences with the classical approach of explicit smoothing are 1) the values of the smoothing coefficient are calculated and not chosen a priori, 2) the magnitude of artificial dissipation is bounded, 3) the values change dynamically during the computation, 4) separate values are employed for each one of the governing equations, and 5) the values can change spatially instead of the same value being employed everywhere in the computational domain.

Received Aug. 8, 1994; revision received Dec. 14, 1994; accepted for publication Dec. 22, 1994. Copyright © 1995 by the American Institute of Aeronautics and Astronautics, Inc. All rights reserved.

*Associate Professor, Department of Aerospace Engineering and Engineering Mechanics. Member AIAA.

†Undergraduate Research Assistant, Department of Aerospace Engineering and Engineering Mechanics.